Available online at www.sciencedirect.com
ScienceDirect
European Journal of Pharmaceutics and Biopharmaceutics 66 (2007) 268–280
European Journal of Pharmaceutics and Biopharmaceutics
www.elsevier.com/locate/ejpb

Research paper

Effect of poly(ethylene glycol)-block-polylactide nanoparticles on hepatic cells of mouse: Low cytotoxicity, but efflux of the nanoparticles by ATP-binding cassette transporters

Yangde Zhang [a,1], Zhiyuan Hu [a,*,1], Maoying Ye [b], Yifeng Pan [a], Jiji Chen [a], Yulin Luo [a], Yanqiong Zhang [a], Lianxiang He [a], Jiwei Wang [a,*]

[a] *Department of Biomedical Engineering, Central South University, Changsha, China*
[b] *Department of Anesthesiology, Central South University, Changsha, China*

Received 25 June 2006; accepted in revised form 7 November 2006
Available online 15 November 2006

Abstract

The objective of this paper is to study the effects of poly(ethylene glycol)-block-polylactide (PLA–PEG) nanoparticles on hepatic cells of mouse. Blank PLA–PEG nanoparticles have been successfully prepared and MTT assay suggested that the nanoparticles with HepG2 cell co-culture model did not cause significant changes in membrane integrity in controlled concentration range (0.001–0.1 mg/ml). Immunohistochemical analysis demonstrated that large dose of PLA–PEG nanoparticles injection (42.04 mg/kg, i.v.) did not induce hepatic cell apoptosis. From biochemical assay experiments, although the levels of SOD decreased and those of MDA, NOS increased after treatment with large dose of PLA–PEG nanoparticles injection (42.04 mg/kg, i.v.), they were all not significant ($p > 0.05$). Then Kunming mice were treated with large dose of PLA–PEG nanoparticles (42.04 mg/kg, i.v.) and after 4 days total RNA was isolated to elucidate patterns of gene expression using a mouse cDNA-microarray (SuperArray). Treatment with nanoparticles resulted in over-expression of a lot of ATP-binding cassette (ABC) transporters, especially two ABC transporters (ABCA8 and ABCC5/MRP5), and down-regulation of GSTP1, in comparison with the control. ABCA8 could extrude low molecular weight polymers after PLA–PEG nanoparticles hydrolysis outside the cells. We also discovered that ABCC5 expressed multidrug resistance protein 5 (MRP5) to pump out conjugate (GS-X) of PLA–PEG nanoparticles with GSH. The results were confirmed by RT-PCR. Results of *in vitro* accumulation and efflux experiments indicated that about 51–52% (51.5% and 52.0%) intracellular PLA–PEG nanoparticles was expulsed after mouse primary hepatocytes reached a saturation uptake of nanoparticles during the concentration range of 750–1000 μg/ml. The results suggested that ABC transporters (especially ABCA8) pump out the polymers after hydrolysis from mouse hepatic cells and large dose of PLA–PEG nanoparticles make mouse hepatic cells gain drug resistance to PLA–PEG nanoparticles.

Keywords: PLA–PEG nanoparticles; ATP-binding cassette transporter; Transport; Efflux; Drug resistance

1. Introduction

In recent years, scientists have prepared a lot of colloidal drug carriers with prolonged blood circulation times. Among them, PEG-coated biodegradable nanoparticles have appeared to be particularly promising drug carriers.

Much attention has been paid to the PLA–polyethylene glycol block copolymer (PLA–PEG), which is a diblock copolymer with hydrophilic and hydrophobic blocks,

Abbreviations: SOD, superoxide dismutase; MDA, malondialdehyde; NOS, nitric oxide synthases; NO, nitric oxide; GSH, glutathione; GS-X, GSH conjugate; MDR, multidrug resistance; P-gp, P-glycoprotein; ABC, ATP-binding cassette.

* Corresponding authors. Department of Biomedical Engineering, National Hepatobiliary and Enteric Surgery Research Center, Central South University, Changsha 410008, China. Tel.: +86 731 4327972; fax: +86 25 4327987.
E-mail addresses: huzhiyuanyamaha@yahoo.com.cn (Z. Hu), jw_wang66@yahoo.com (J. Wang).

[1] These authors contributed equally to this work.

0939-6411/$ - see front matter © 2006 Elsevier B.V. All rights reserved.
doi:10.1016/j.ejpb.2006.11.003

because it allows the formation of a stable nano-particulate suspension in an aqueous solvent, where PLA chains form the core and PEG chains are located outside [1]. The PEG shell prevents the interaction of PLA core with biomolecules, cells and tissues, and can suppress opsonization [2]. Reportedly, PLA–PEG nanoparticles show a particle size of several dozen to a few hundred nanometers, and possess a hydrophilic and inactive surface of PEG, leading to a longer systemic circulation [3,4]. PLA–PEG particles with a high PEG coating density and a small size were more significantly transported than noncoated PLA nanoparticles and also than PLA–PEG nanoparticles with a lower coating density [5].

A lot of research suggested that bulk PLA–PEG or PLA–PEG/hydroxyapatite composite used in bone induction and bone repair have satisfactory biocompatibility [6–8]. But properties of PLA–PEG nanomaterials with at least one dimension of 100 nm or less differ from those of bulk PLA–PEG materials. There are several unusual physicochemical properties of nanoparticles, of course including PLA–PEG nanoparticles. The main property of nanoparticles is their size, which falls in the transitional zone between individual atoms or molecules and the corresponding bulk materials. So the uptake and interaction of nanoparticles with biological tissues increase overwhelmingly. This effect can generate different biological effects in living cells that would not otherwise be possible with the same material in larger form. Surface area is another important characteristic of nanoparticles. The increase in surface area determines the potential number of reactive groups on the particle surface. So nanoparticles easily deposit in target organs, penetrate cell membranes, lodge in mitochondria. Possible different results of these capabilities are interactions with biological systems. Some studies suggest that several nanomaterials affect biological behaviors at the cellular, subcellular, and protein levels [9–12].

The possible mechanisms for the particles to pass through the physiological barriers could be endocytosis uptake – particles absorbed by cell through endocytosis (particle size < 500 nm) [13]. Confocal microscopy demonstrated that PLGA nanoparticles were internalized by human arterial vascular smooth muscle cells (VSMCs) rapidly within 1 min after incubation. However, once the extracellular nanoparticle concentration gradient was removed, exocytosis of nanoparticles occurred with about 65% of the internalized fraction in 30 min [14]. Poly(ethylene glycol) (PEG)-coated particles can greatly improve their adhesion to and absorption into the intestinal cells (for example Caco-2 cells) as well as the ability to escape from the multidrug resistance pump proteins by suppressing intestinal P-glycoprotein (P-gp) function [15–17]. P-gp belongs to the superfamily of ATP-binding cassette (ABC) transporters.

The ABC transporters belong to the largest known transporter gene family. These intracellular and extracellular membrane-spanning proteins translocate a variety of substrates including sugars, amino acids, metal ions, peptides, proteins, and hydrophobic compounds across cellular compartments. One largest sub-family of the ATP-binding cassette (ABC) transporters able to affect drug disposition is the ABCC (multidrug resistance-associated protein, MRP) family. The MRPs can transport a large range of organic anions, including anionic drugs and drugs conjugated to glutathione (GSH), sulfate, or glucuronate.

The liver is the largest internal organ in vertebrates, including human. Hepatic cells carry out more chemical processes than any other group of cells in vertebrate's body. The hepatic cells break down most medicinal products in a process called drug metabolism [18]. PLA–PEG nanoparticles exhibited increased plasma circulation times and reduced liver accumulation in mice. But *in vivo* experiments showed that the concentration of PLA–PEG nanoparticles in mice liver 6 h after intravenous injection of this nanoparticle solution was still high (9.1%). The PLA–PEG nanoparticles still exhibited major liver accumulation in mice [19]. So the mouse liver is very important in PLA–PEG nanoparticles metabolism.

In this study, we concentrated on examining the effect of blank PLA–PEG nanoparticles on hepatic cells of mouse. One goal of the current study was to determine the effect of PLA–PEG nanoparticles on hepatic cells, gene expression in mouse, especially gene expression of many ATP-binding cassette (ABC) transporters. In the present work, we also found the possible mechanisms of several ABC transporters on PLA–PEG nanoparticles transport through hepatic cell membrane. This study may contribute to a better understanding of the effect mediated by PLA–PEG nanoparticles.

2. Materials and methods

Poly(ethylene glycol)-block-polylactide (PLA–PEG; MW 30 kDa), Pluronic F-68 (MW 2000) and MTT were purchased from Sigma–Aldrich Co. (USA). Acetone (purity $\geqslant 99.5\%$) and 6-coumarin were obtained from Sinopharm Chemical Reagent Co., Ltd. (Beijing, China). *In Situ* Cell Apoptosis Detection Kit II was purchased from Wuhan Boster Inc. (Wuhan, China). The assay kits for MDA, NOS, SOD, and Coomassie brilliant blue protein were purchased from Jiancheng Biologic Project Company (Nanjing, China). All other reagents used were of analytical grade.

2.1. Preparation of blank PLA–PEG nanoparticles and PLA–PEG nanoparticles containing 6-coumarin as a fluorescent marker

Blank PLA–PEG nanoparticles were prepared using an oil-in-water emulsion-solvent evaporation method. We optimized the nanoparticles preparation method by the Uniform Design method described in our previously published paper [20]. For this method, a $U_{12}(2^6)$ factorial design was assessed, where 6 refers to the number of main factors on nanoparticles preparation, 2 refers to the

number of levels for each factor, and 12 refers to the number of experiments. Briefly, 30 mg of PLA–PEG was fully dissolved in 10 ml acetone by stirring magnetically (Constant Temperature Magnetic Stirring Instrument, Huhua, China). The organic phase of acetone was added into a volume of 20 ml of a 0.5% (w/v) Pluronic F-68 aqueous solution, and the two phases were emulsified for 1.5 min with a high speed homogenizer (ULTRA-TURRAX T-25 Basic, IKA, Germany). The organic solvent was then eliminated by evaporation below 60 °C. Finally, the particles were isolated by centrifugation (3K18, Sigma, Germany, 10,000 rpm, 25 min) and washed three times with water to give suspension of the particles. The PLA–PEG nanoparticles containing 6-coumarin as a fluorescent marker were prepared by using the same method as the blank PLA–PEG nanoparticles preparation, but adding 50 μg 6-coumarin into PLA–PEG acetone solution. The blank PLA–PEG nanoparticles and PLA–PEG nanoparticles containing 6-coumarin were then lyophilized (Labconco®, Kansas, USA) for 48 h to obtain dry powder.

2.2. Physicochemical and morphological characterization of nanoparticles

The particle sizes, polydispersity and ζ potential of nanoparticles were determined by Zetasizer® 1000HSA Laser particle analyzer (Malvern Instruments, UK), in triplicate. The surface morphology of the nanoparticles was observed using a JEOL JSM-6360LV scanning electron microscope (SEM) at 20.0 kV. The samples were mounted onto stubs by means of quick drying silver paint, and then coated with gold palladium to a thickness of approximately 25 nm.

2.3. Cell line and animals

Human hepatoma (HepG2) cells were obtained from the Centralab of the Xiangya hospital, Central South University. Cells were cultured in RPMI-1640 medium (Gibco Life Technologies) enriched with 10% heat-inactivated fetal calf serum (Min Hai Co. Ltd., Qinghai, China) and 1% penicillin/streptomycin (Gibco Life Technologies), and incubated under standardized conditions (37 °C, 5% carbon dioxide, 100% humidity). Female Kunming mice (Animal Center of Central South University, China), weighing 18–20 g, were housed in a pathogen-free animal facility and given commercial basal diet.

For the primary culture of mouse hepatocytes, three Kunming female mice were anesthetized with 1.5 ml/kg of nembutal sodium solution containing 50 mg/ml of pentobarbital sodium prior to undergoing liver perfusion. All animals used in this study were handled in accordance with the principles and guidelines prepared by our Institutional Animal Care and Use Committee. Mouse primary hepatocytes were isolated by a two-stage collagenase perfusion process according to the methods described by Seglen and Kreamer [21]. Primary hepatocytes were suspended in L-15 medium (Gibco Life Technologies) containing 2 mg/ml BSA, 18 mM Hepes, 3 mg/ml proline, 1 mg/ml galactose, 0.1% insulin-transferrin-selenite, 10 ng/ml epidermal growth factor, 50 U/ml penicillin, and 50 μg/ml streptomycin.

2.4. MTT assay

MTT (tetrazolium salt) assay was applied to evaluate the effect of PLA–PEG nanoparticles on HepG2 cell viability by measuring the uptake and reduction of tetrazolium salt to an insoluble formazan dye by cellular microsomal enzymes [22]. HepG2 cell suspensions (200 μl; 1×10^5 cells) were dispensed (two wells for each particle type) into 96-well plates (Helena BioSciences, UK) and incubated overnight (16 h) to allow for cell adherence. Culture medium was replaced with 200 μl of PEG–PLA particles/culture medium suspensions with different concentrations of 0.001, 0.005, 0.01, 0.03, 0.06, 0.09, and 0.10 mg/ml and incubated at 37 °C for 24 h. HepG2 cells without nanoparticles were used as the control. Next, 100 μl of MTT (1 mg/ml) solution was added into each well and was allowed to react at 37 °C for 4 h. The solution was removed and 150 μl of dimethylsulfoxide (DMSO) was added into each well. Then the plate was incubated for 30 min at room temperature. Absorption at 490 nm was measured with Microplate Reader 3550 (Bio-Rad, USA). The cell viability was calculated by the following formula: cell viability (%) = optical density (OD) of the treated cells/OD of the nontreated cells.

2.5. Animal treatment schedules: nanoparticles intravenous injection

The experimental procedures and housing conditions were approved by our Institutional Animal Care and Use Committee, and all animals were cared for and treated humanely in accordance with our institutional guidelines on animal experimentation. Mice were housed in groups of 4 per cage with free access to food and water for 2 d before the experiment. Kunming mice were randomized into groups, as follows. Large dose treatment group: four 18–20 g Kunming mice received PLA–PEG nanoparticles sterilizing ddH_2O solution injection via the tail vein (42.04 mg/kg, i.v.) and were killed after 4 days. Control group: another 4 mice with no treatment were housed to a cage with the same breeding as the treatment group. The large dose injection was determined by the LD_{50} (15.06 mg/kg) of epirubicin i.v. in mouse and the drug-loaded ratio (8.22%) of epirubicin-loaded PLA–PEG nanoparticles obtained from former experiment (0.8408 mg PLA–PEG nanoparticles for a 20 g mouse) [20]. All mice of two groups were sacrificed for the next experiments after 4 days.

2.6. Immunohistochemical analysis of tissues

Mice were killed and small pieces of liver, heart, and kidney were obtained after they were treated with large dose of PLA–PEG nanoparticles (42.04 mg/kg, i.v.). Four mice

receiving 9.43 mg/kg body weight of As_2O_3 (LD_{50} of mice) subcutaneous injection served as control. Small pieces of liver, heart, and kidney from As_2O_3 injection mice were also obtained after 4 days. Small pieces from PLA–PEG nanoparticles treated mice and As_2O_3 treated mice were fixed by 10% formalin and then embedded into paraffin, sectioned for 5 μm thick, and mounted on the glass microscope slides using standard histopathological techniques. Paraformaldehyde-fixed tissue sections were dewaxed according to standard procedures. Slides were presoaked in 3% (v/v) acetic acid for 10 min, then incubated with protease K (20 μg/ml) for 15 min at 37 °C. Slides were incubated in labeling buffer (1 μl TdT + 1 μ LDIG-d-UTP per 1 slide) for 2 h at 37 °C. After the TdT reaction, sections were soaked in TdT blocking buffer. Actin-DIG-Biotin was added into slides and incubated for 1 h. Then SABC-AP was added into slide to react with actin-DIG-Biotin. Then they were stained with BCIP/NBT. Nuclei were counterstained with hematoxylin and examined by light microscopy.

2.7. SOD, NOS, and MDA activity assay

Mice from nanoparticles-treated group and control group were sacrificed after 4 days, blood was drawn by cardiac puncture into a syringe and removed to a test tube. Serum was separated by centrifugation at 3000 rpm for 5 min within 2 h of being drawn and was stored at −30 °C for not more than 2 days before analysis. Whole liver, heart, and kidney were quickly removed on an ice-plate, and washed with cold 0.9% saline solution. Three samples were, respectively, homogenized in 0.9% saline solution using a motor-driven homogenizer. The homogenate was then centrifuged for 10 min at 3000 rpm at 4 °C in a Sigma centrifuge (Model 3K18). The supernatant obtained was used for assays of SOD, NOS and MDA activities using commercial kits, respectively. The optical density was read on a Hitachi spectrophotometer (Model U-3000, Japan). Total (Cu–Zn and Mn) SOD activity was determined according to the method of Sun et al. [23]. The MDA level was determined by a method based on the reaction with thiobarbituric acid (TBA) at 90–100 °C [24]. Protein concentrations were estimated using the Diagnostic Reagent Kit (Coomassie protein assay dye) [25].

2.8. cDNA gene expression array analysis

GEArray Q series Mouse Drug Metabolism Gene Array (Cat No: M-011, SuperArray) contains 96 genes critical in the drug metabolism process. The genes encoding enzymes that are important for drug transport, phase I metabolism, and phase II metabolism are represented on the array. Each GEArray Q Series membranes are spotted with negative controls (pUC18 DNA and blanks) and housekeeping genes. A complete gene list is available at website www.superarray.com. Total RNA of mouse liver was isolated using TRIZOL Reagent (Invitrogen Life Technologies) and quantified spectrophotometrically (DU1 640, Beckman, USA). Liver samples from PLA–PEG nanoparticles treated group (4 mice) were mixed together; mixed sample was homogenized in 1 ml of TRIZOL Reagent per 50–100 mg of tissue using a power homogenizer (ULTRA-TURRAX T-25 Basic, IKA, Germany). The same was done for liver samples from the control group (4 mice). The biotin-16-dUTP-labeled cDNA probes were synthesized from 5 μg of total RNA according to instruction from the manufacturer. After pre-hybridization with GEAhyb Hybridization Solution (SuperArray) containing 100 μg of DNA/ml of denatured salmon sperm DNA (Invitrogen) for 2 h at 60°C, the array membrane was hybridized with denatured cDNA probes overnight at 60 °C. Following washing the membrane twice with 2 × SSC, 1% SDS and twice with 0.1 × SSC, 0.5% SDS for 15 min at 60 °C each, the membrane was blocked with GEAblocking Solution Q (SuperArray) for 40 min and incubated with alkaline phosphatase-conjugated streptavidin for 10 min at room temperature. Chemiluminescent detection was performed using CDP-Star substrate. The image obtained using desktop scanner was analyzed with ScanAlyze software. The intensity of each signal was normalized against that of GAPDH on the array. GEArray Analyzer software was used to background subtraction and data normalization. We filtered up-regulated genes as their fold change $\geqslant 2$, and filtered down-regulated genes as their fold change $\leqslant 0.5$ (fold change = normalized result of treatment group/normalized result of the control group).

2.9. Semiquantitative RT-PCR

We used Robust™ I RT-PCR Kit (Finnzymes, Finland) in this study.

We added the following reaction components into a nuclease-free PCR tube; 5 μl of 10 × RobusT Reaction Buffer, 1.5 μl of 50 mM $MgCl_2$, 1 μg of total RNA, 1 μl dNTP, 10 pmol of down primer, 10 pmol of upstream primer, 1 μl of M-MLV reaction buffer and 2 μl DyNAzyme EXT DNA Polymerase, then added RNase-free H_2O to 50 μl. The thermal cycling parameters consisted of cDNA synthesis at 45 °C for 40 min, inactivation of AMV Reverse Transcriptase at 94 °C for 2 min, denaturation at 94 °C for 30 s, annealing at 52 °C for 30 s and extension at 72 °C for 60 s for 30 cycles followed by extension at 72 °C for 8 min. After amplification the samples were separated on a 1% agarose gel containing 0.3 μg/ml of ethidium bromide and bands visualized and photographed using a translucent UV source. The stained image was recorded and the band intensity was quantified using densitometric analysis by Sigma Gel Software (SPSS). The mRNA level was expressed as a ratio to actin beta. The following murine oligonucleotide primers (5′–3′ sequences) were used for RT-PCR analysis: ABCA8 sense, TGGAACGCCAGAACATAG; ABCA8 antisense, GTAAGCCGAAGGGAAGAG; GSTP1 sense, CTGGA AGGAGGAGGTGGT; GSTP1 antisense, GCATTAG ATTGGTAAAGGGT; ABCC5 sense, CCTGCCA

GAATCAAGAAC; ABCC5 antisense, CGTCCCAC AATGCCTATC; Mouse actin beta sense, GTCCC TCACCCTCCCAAAAG; Mouse actin beta antisense, GCTGCCTCAACACCTCAACCC.

2.10. Accumulation and efflux assays

For accumulation studies mouse primary hepatocytes were plated in triplicate at a density of 5×10^5 cells per well of a poly (L-lysine)-treated 12-well plate overnight. Cells were incubated with 0.5 ml of 40, 400, 750, and 1000 μg/ml PLA–PEG nanoparticles containing 6-coumarin fluorescent marker for 2 h at 37 °C in L-15 medium. After nanoparticles accumulation, medium was removed, and cells were washed three times with 2 ml of ice-cold PBS and then lysed by incubating them with 0.1 ml of 1 × cell culture lysis reagent (Promega, Madison, USA) for 30 min at 37 °C. The cell lysates were processed to determine the nanoparticle levels by high-performance liquid chromatography (HPLC) (Shimadzu Scientific Instruments, Columbia, USA) as per J. PANYAM's method [14,26].

For efflux studies, mouse primary hepatocytes were plated in triplicate at a density of 5×10^5cells per well of a poly (L-lysine)-treated 12-well plate overnight. Then cells were incubated with PLA–PEG nanoparticles (40, 400, 750, and 1000 μg/ml) containing 6-coumarin fluorescent marker for 2 h in L-15 medium, followed by washing off of the uninternalized nanoparticles with PBS for two times. The cells in wells were then incubated with fresh growth medium. After 2 h, the medium was removed, cells were washed twice with PBS and lysed, and the intracellular nanoparticle levels were analyzed to obtain the fraction of nanoparticles that were expulsed out of the cells.

2.11. Data analysis

Results are presented as means ± SD (standard deviation). The statistical significance of data from the treated group compared with the control group was analyzed using Paired-Samples *t* test. As usual, the level of significance was set at $p < 0.05$.

3. Results and discussion

3.1. Particle size, ζ potential and morphology of PLA–PEG nanoparticles

The size, polydispersity and ζ potential of blank PLA–PEG nanoparticles and PLA–PEG nanoparticles containing 6-coumarin as a fluorescent marker are presented in Table 1. The size and ζ potential of particles containing 6-coumarin as a fluorescent marker were similar to those of blank particles. The diameter distribution of PLA–PEG nanoparticles prepared by the emulsification techniques was narrow. This is a direct consequence of the nanoparticles' formation process, in the emulsification procedures, the high energy applied (high speed homogenizer) generated droplets of a well-controlled diameter, which became nanoparticles following the solvent evaporation [5]. Well diameter distribution also contributed to the Uniform Design method to plan experiments. The mean ζ potential of blank nanoparticles prepared by the emulsion technique was -20.0 ± 2.1 mV. The low ζ potential of PLA–PEG nanoparticles as compared to that of PLA nanoparticles has been attributed to the shift of the shear plane of the particles due to the presence of the PEG chains on the nanoparticle's surface [27].

The blank PLA–PEG nanoparticles were observed with SEM (Fig. 1). This image was typical of those obtained for all the samples, confirming that the PLA–PEG copolymers form spherical, discrete particles in aqueous media.

3.2. Result of MTT assay

The viability of HepG2 in the presence of PLA–PEG nanoparticles is shown in Fig. 2. The viability, as determined with an MTT assay, was normalized to the viability of cells cultured without nanoparticles, and thus, values

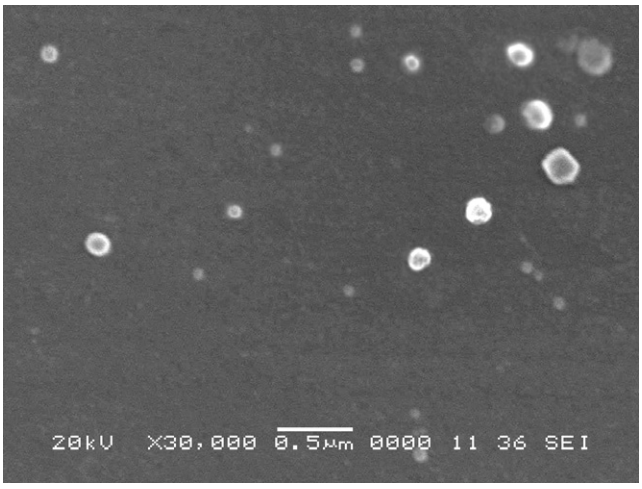

Fig. 1. Scanning electron microscopy (SEM) of PLA–PEG nanoparticles.

Table 1
Physicochemical properties of blank PLA–PEG nanoparticles and PLA–PEG nanoparticles containing 6-coumarin as a fluorescent marker

Nanoparticles	Particle size (mean ± SD) (nm)	Polydispersity (mean ± SD)	ζ Potential (mean ± SD) (mV)
Blank PP NP[a]	157 ± 16	0.32 ± 0.05	−20.0 ± 2.1
PP (6-coumarin)[b]	165 ± 9	0.30 ± 0.0	−18.8 ± 1.6

[a] Blank PP NP: blank PLA–PEG nanoparticles.
[b] PP (6-coumarin): PLA–PEG nanoparticles containing 6-coumarin.

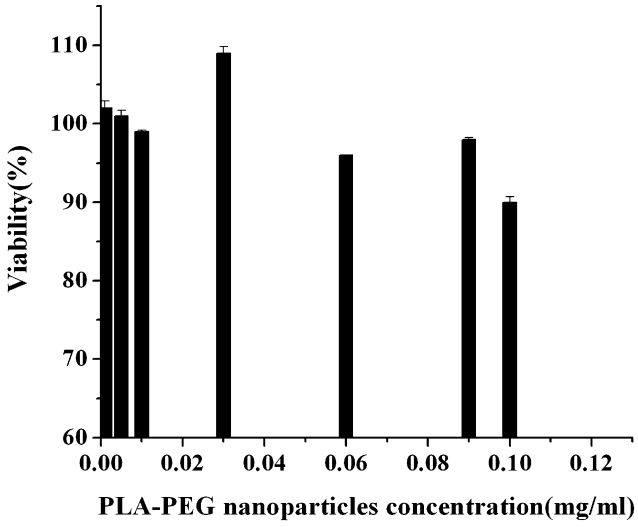

Fig. 2. MTT assay results.

close to 1 are indicative of nontoxic cell culture conditions. The results of MTT assays showed PLA–PEG nanoparticles exposure exhibited no obvious cytotoxicity from 0.001 to 0.1 mg/ml. More than 90% of cells were viable after treated with nanoparticles from 0.001 to 0.1 mg/ml. So PLA–PEG nanoparticles might be recognized as biocompatible in a large concentration range. Lin et al. showed the cytotoxicity in terms of cell viability after treated with PLA–PEG micelles was insignificant from 0.001 to 0.1 mg/ml [28]. The result suggested that the nanoparticles with the cell culture model did not cause significant changes in membrane integrity in controlled concentration range.

3.3. No apoptotic cells in immunohistochemical slides

Microphotographs of liver sample, kidney sample and cardiac samples (Fig. 3) stained for TUNEL apoptotic cell, detection in nanoparticles treated group indicated that large dose of PLA–PEG nanoparticles injection did not induce cell apoptosis. Apoptotic cells presented yellow brown staining after BCIP/NBT coloration in TUNEL staining. In positive control, TUNEL-positive cells were detected in liver, kidney, and heart sections of As_2O_3 LD_{50} dose treated mice (Fig. 3).

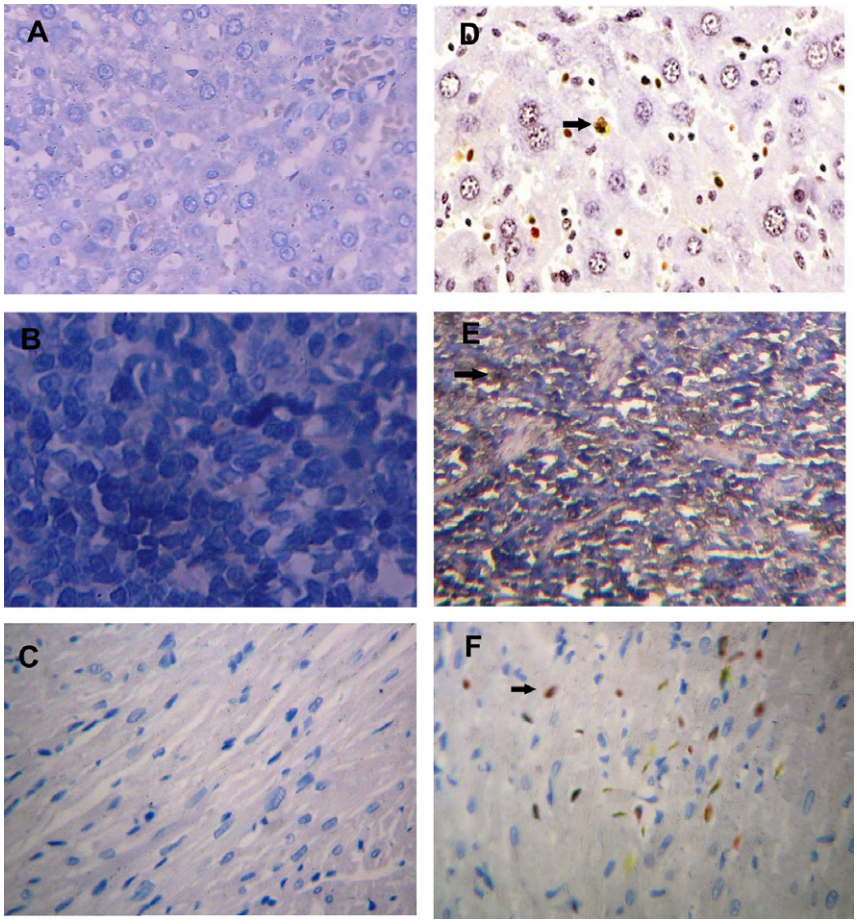

Fig. 3. Microphotographs of liver sample (A) (magnification 400×), kidney sample (B) (magnification 400×) and cardiac samples (C) (magnification 400×) stained for TUNEL apoptotic cell detection in nanoparticles treated group. The sections were stained with hematoxylin. We did not find apoptotic cells which presented yellow brown staining. Figures with positive control inducing apoptosis (arrow, yellow brown) after As_2O_3 injection: liver sample (D) (magnification 400×), kidney sample (E) (magnification 200×) and cardiac samples (F) (magnification 400×). (For interpretation of the references to colour in this figure legend, the reader is referred to the web version of this article.)

3.4. The effects of PLA–PEG nanoparticles on the levels of superoxide dismutase, malonaldehyde, and nitric oxide synthase in mice

The effects of large dose injection of PLA–PEG nanoparticles on the levels of superoxide dismutase (SOD), malonaldehyde (MDA), and nitric oxide synthetase (NOS) in mice are given in Table 2. Some changes in the activities of SOD and NOS enzymes and MDA level of liver, kidney, heart, and serum were observed between large dose treated group and the control group; however, there was no statistical significance among two groups ($p > 0.05$) (Table 2). SOD of liver, kidney, heart, and serum in the large dose treated group decreased 2.75% ($p > 0.05$), 2.48% ($p > 0.05$), 1.49% ($p > 0.05$), and 1.31% ($p > 0.05$), respectively, compared with that of control group. They were all not significant ($p > 0.05$). The increases of MDA of liver, kidney, heart, and serum (4.21%, 3.63%, 4.60%, and 8.12%, respectively) in the large dose treated group compared with that of control group were also not significant ($p > 0.05$). NOS of liver, kidney, heart, and serum in treated group increased 6.97% ($p > 0.05$), 9.30% ($p > 0.05$), 2.62% ($p > 0.05$), and 9.13% ($p > 0.05$), respectively, compared with that of control group. Oxygen radicals would harm cells and MDA, as a kind of lipid peroxidation, would reflect the degree of oxidation in the body. SOD is a scavenger of free radicals, which has important effects in the control of oxidation reactions in the body. NOS can produce an endothelial-enlarging factor NO by catalyzing L-arginine. Excessive NO is pathogenic. From these experiments, although the levels of SOD decreased and levels of MDA, NOS increased after treatment with large dose of PLA–PEG nanoparticles injection, they were all not significant ($p > 0.05$). The results suggested that large dose of PLA–PEG nanoparticles injection did not induce cell damage of liver, kidney, heart, and serum.

3.5. Results of in vitro accumulation and efflux study

In vitro accumulation studies indicated that nanoparticle uptake was concentration-dependent (Fig. 4). The PLA–PEG nanoparticle uptake increased rapidly during the concentration range of 40–750 μg/ml, and reached a saturation uptake rate from 750 to 1000 μg/ml. In the efflux studies, after the removal of PLA–PEG nanoparticles from the medium, about 52.0% (466.20/896.5) of the internalized nanoparticles were expulsed by mouse primary hepatocytes for 1000 μg/ml dose in 2 h, 51.5% (453.52/880.17), 26.5% (144.07/544.62), and 21.3% (16.35/76.64), respectively, for 750 μg/ml dose, 400 μg/ml dose, and 40 μg/ml dose. The results indicated that when mouse primary hepatocytes reached a saturation uptake of PLA–PEG nanoparticles, about 51–52% (51.5% and 52.0%) intracellular nanoparticles was expulsed by mouse primary hepatocytes during the concentration range of 750–1000 μg/ml.

3.6. Microarray analysis of mice liver treated with blank PLA–PEG nanoparticles

3.6.1. Gene expression change

Fig. 5 shows the results of the array experiment and Table 3 shows the genes that were induced significantly (fold change $\geqslant 2$ or fold change $\leqslant 0.5$, $p < 0.05$) by the nanoparticles. Function groups included ATP-binding cassette (P-gp), P450 Gene Family (Table 3). The β-actin gene was included on the array in row 17, columns 7 and 8. No increase in β-actin gene expression was observed in the nanoparticles treated liver.

3.6.2. Efflux of polymers after nanoparticles hydrolysis by ATP-binding cassette (ABC) transporters

ATP-binding cassette (ABC) transporters are an extended family of membrane proteins defined by a highly

Table 2
Effects of treatment with PLA–PEG nanoparticles on SOD and NOS activities and MDA level of tissue and serum in control and treated mice

Group	MDA (nmol/mgprot for organ, nmol/ml for serum)	SOD (U/mgprot for organ, U/ml for serum)	NOS (U/mgprot for organ, U/ml for serum)
Heart			
Control	0.87 ± 0.06	192.27 ± 4.75	4.97 ± 0.25
Treated	$0.91 \pm 0.09^{*}$	$189.39 \pm 3.61^{*}$	$5.10 \pm 0.68^{*}$
Liver			
Control	4.51 ± 0.06	174.40 ± 9.78	6.46 ± 0.15
Treated	$4.70 \pm 0.02^{*}$	$171.60 \pm 7.67^{*}$	$6.91 \pm 0.16^{*}$
Kidney			
Control	3.03 ± 0.05	205.93 ± 2.79	5.57 ± 0.56
Treated	$3.14 \pm 0.06^{*}$	$202.81 \pm 2.06^{*}$	$5.97 \pm 0.89^{*}$
Serum			
Control	9.85 ± 0.23	121.48 ± 1.60	10.19 ± 1.58
Treated	$9.93 \pm 0.46^{*}$	$119.88 \pm 1.07^{*}$	$11.12 \pm 2.12^{*}$

Mice were dosed with large dose PLA–PEG nanoparticles (treated) and the control as described in the experiment details section. Data are expressed as means ± SD ($n = 7$).

* $p > 0.05$ as compared to control of each group.

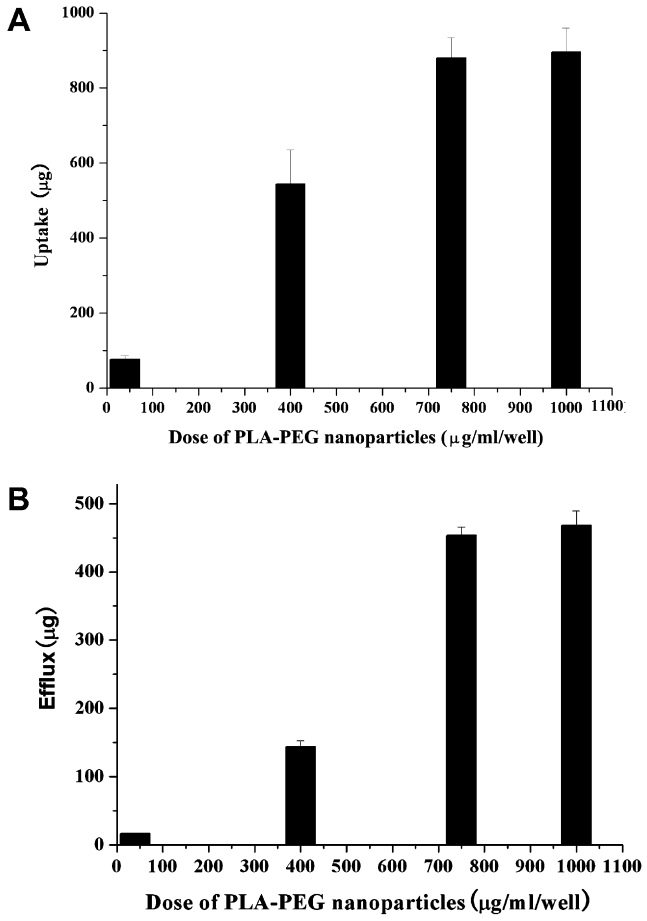

Fig. 4. Dose-dependent uptake of PLA–PEG nanoparticles. Mouse primary hepatocytes were incubated with different doses of nanoparticles for 2 h (A), and cells reached a saturation uptake rate from 750 to 1000 μg/ml. Efflux of nanoparticles from hepatocytes after nanoparticles containing medium removed (B). After cells reached a saturation uptake of nanoparticles, about 51–52% of internalized nanoparticles were expulsed from cells. Data as means ± SD, $n = 3$.

conserved domain, the ATP-binding cassette. They mediate the ATP-dependent transport of a wide variety of compounds across cellular membranes [29,30]. The gene expression resulting from array experiment showed a lot of up-regulated genes expressed ATP-binding cassette (ABC) transporter proteins (ABCA2, ABCA7, ABCA8, ABCC9, ABCD1, ABCD3, ABCD4, ABCF1, and ABCF3). The genes of ATP-binding cassette significantly overexpressed (fold change $\geqslant 2$) are shown in Table 3. In these genes, ABCA8 showed the highest difference (fold change = 269.70).

After mice received large dose of PLA–PEG nanoparticles solution injection (42.04 mg/kg, i.v.) a lot of PLA–PEG nanoparticles were internalized by hepatic cells rapidly. At the same time more and more PLA–PEG nanoparticles were still internalized by mouse hepatic cells endlessly as the PLA–PEG nanoparticles exhibited long blood circulation. *In vitro* accumulation experiments also indicated that the uptake of PLA–PEG nanoparticles by mouse liver cells increased rapidly as the concentration of nanoparticles in culture medium increased. The cells could reach a saturation uptake of nanoparticles in certain concentration range (750–1000 μg/ml). Degradation of PLA or PLA–PEG occurs by autocatalytic cleavage of the ester bonds through spontaneous hydrolysis into oligomers and D, L-lactic acid. Lactate converted into pyruvate enters the Krebs' cycle to be degraded into CO_2 and H_2O [31]. Former studies found that after intravenous administration of ^{14}C-$PLA_{18,000}$ radiolabeled nanoparticles to rats, the ^{14}C-labeled polymer was rapidly captured by liver, the PLA nanoparticles spontaneously hydrolyzed into oligomers, and then proceeded to lactic acid which is rapidly converted into CO_2 and H_2O via the Krebs' cycle, 80% of the recovered ^{14}C as CO_2 was eliminated [32]. PEG–PLA nanoparticles have similar degradation behaviors [33]. *In vivo* experiments of PLA/PLA–PEG membrane nanoartificial red blood cells indicated that these polymers were degraded into lactic acid and then water and carbon dioxide [34,35]. The Krebs' cycle reactions take place in the matrix of the mitochondria. The mitochondrial matrix contains pyruvate dehydrogenase and enzymes of Krebs' cycle. Intracellularly delivered polymer nanoparticles must be degraded in targeted cells in order to release incorporated drug. Internalized PLA–PEG nanoparticles were hydrolyzed into oligomers by cleavage of the ester bonds in order to release loaded drug. Hepatic cells would be filled with low molecular weight polymers after hydrolysis as mouse hepatic cells reached saturation uptake of PLA–PEG nanoparticles. A part of polymers proceeded to lactic acid which was converted into pyruvate by the catalysis of cytoplasmic lactate dehydrogenase (LDH), as cytoplasm of mouse liver cells contains a lot of LDH [36]. Then pyruvate entered into mitochondrial matrix and proceeded into the Krebs' cycle. But a lot of polymers after hydrolysis must be pumped out of hepatic cells in order to maintain normal physiologic function of cells. Microarray analysis showed that after large dose of PLA–PEG nanoparticles administration, a lot of ATP-binding cassette (ABC) transporters over-expressed, especially ABCA8. We suggested that these ABC transporters (especially ABCA8) were responsible for the efflux of polymers after nanoparticles hydrolysis from the cells. Model (Fig. 6) depicted ABC transporters transport polymers after nanoparticles hydrolysis across mouse hepatic cell membrane.

Among all up-regulated ATP-binding cassette genes, ABCA8 showed the highest difference. This protein is a member of the ABC1 subfamily. The function of this protein has not been clear. Wakaumi et al. investigated the roles of this transporter ABCA8 of mouse; the results suggested that ABCA8 plays a role in digoxin metabolism in the liver. It was found that mouse ABCA8 was mainly expressed in the liver and heart of mouse, similar to human ABCA8 [37]. The up-regulation of the ABCA8 mRNA expression in the liver 4 days after injection was further confirmed by quantitative reverse transcription-PCR (Fig. 7, Table 4). The results suggested that ABCA8 over-expressed after large dose of PLA–PEG nanoparticles

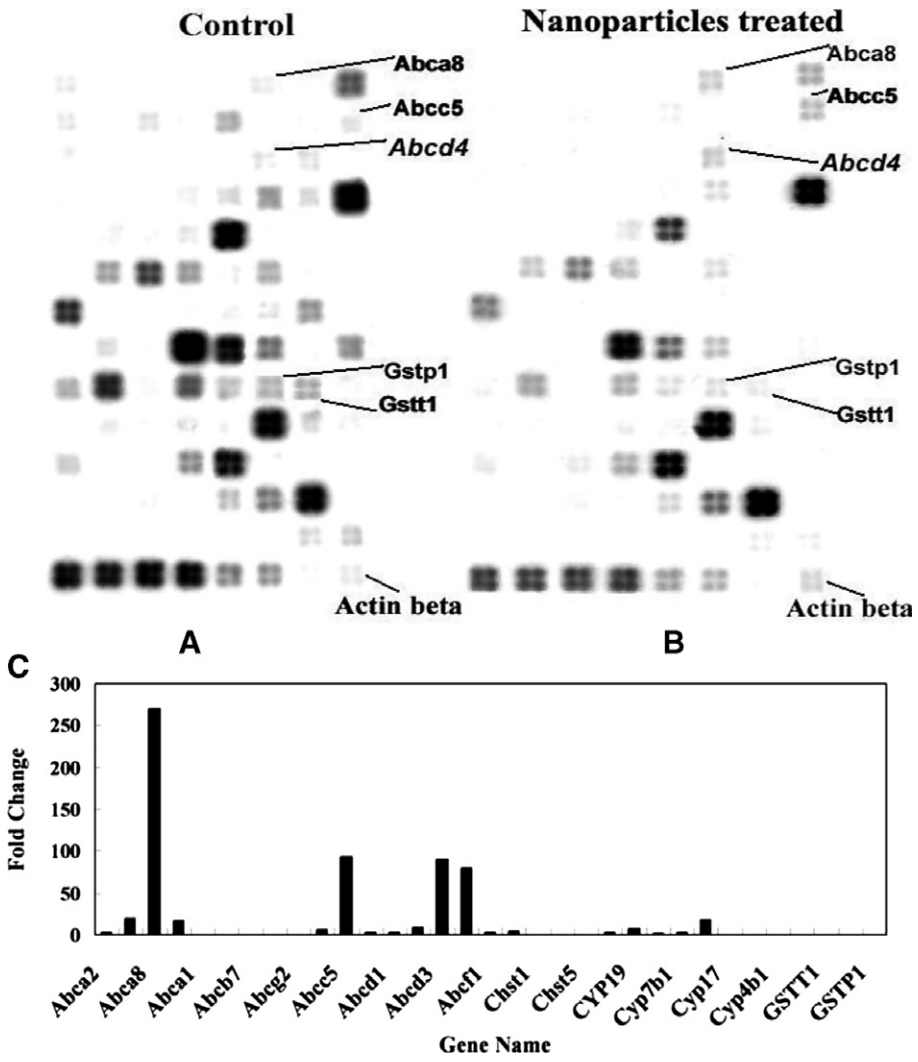

Fig. 5. Pictures of cDNA membrane analyzing gene expression of mouse liver. (A) The control. (B) Mouse treated with large dose of PLA–PEG nanoparticles. (C) Gene expression (only genes modulated by factors of $\geqslant 2$ or $\leqslant 0.5$-fold) fold changes histogram of mice treated with PLA–PEG nanoparticles (42.04 mg/kg, 4 days) and the control.

administration. ABCA8 may play an important role in blank PLA–PEG nanoparticles metabolism in mouse liver.

3.6.3. Efflux of PLA–PEG nanoparticles by ABCC5 (MRP5)

Unlike P-glycoprotein, MRPs are organic anion transporters; they transport anionic drugs, exemplified by methotrexate, and neutral drugs conjugated to acidic ligands, such as glutathione (GSH), glucuronate, or sulfate. But the physiologic function of MRP5 is not known [38,39]. The location of ABCC5 (MRP5) in the canalicular membrane of the hepatocytes helps to clear drugs from the body [39]. MRP5 actively transported conjugated organic anions such as the endogenous glutathione conjugate cysteinyl leukotriene C4 and glutathione-conjugated aflatoxin B1 [40]. Wijnholds et al. reported that human multidrug resistance 1 (MRP5) P-glycoprotein could mediate the cellular extrusion of xenobiotics from normal cells. They found resistance against the thiopurine anticancer drugs, 6-mercaptopurine (6-MP) and thioguanine, and the anti-HIV drug 9-(2-phosphonylmethoxyethyl) adenine (PMEA) in MRP5-transfected 293 Human Embryonic Kidney (HEK) cells [38]. Confocal imaging of HEK293 cells expressing a green fluorescent protein-ABCC5 construct displayed highest fluorescence at the plasma membrane, overexpression of pABC11 (ABCC5) resulting in anionic fluorochromes' efflux from HEK293 cells [41]. Rappa et al.'s observations provided evidence that: baseline MRP5 expression protects cells from the xenobiotics by effluxing the xenobiotics and GSH by a co-transport mechanism [42]. Some drugs can be conjugated to GSH by glutathione *S*-transferase (GST) and are then transported by MRP5.

In ζ potential studies, we found that the ζ potential of blank PLA–PEG particles was -20.0 ± 2.1 mV. High amount of negative charge PLA–PEG nanoparticles was internalized by mouse hepatic cells. A part of negative charge nanoparticles were recognized by cells as xenobiotics and

Table 3
Gene expression (only genes modulated by factors of $\geqslant 2$ or $\leqslant 0.5$-fold) profiling of mice treated with PLA–PEG nanoparticles (42.04 mg/kg, 4 days) and the control

Gene name	GenBank	The control	Nanoparticles treated group	Fold change
Drug transporters: ATP-binding cassette (P-gp)				
ABCA2	NM_007379	0.00522	0.01841	3.53
ABCA7	NM_013850	0.00049	0.00973	19.53
ABCA8	**NM_013851**	**0.00002**	**0.00707**	**269.70**
ABCB2	NM_013683	0.00181	0.02955	16.33
ABCA1	NM_013454	0.04981	0.01575	0.31
ABCB11	NM_021022	0.04774	0.02325	0.49
ABCB7	U43892	0.21296	0.07137	0.34
ABCB9	NM_019875	0.01681	0.00738	0.44
ABCG2	NM_011920	0.04575	0.01414	0.31
ABCB8	AF213391	0.00123	0.00684	5.55
ABCC5	**NM_013790**	**0.00133**	**0.12301**	**92.48**
ABCC9	NM_011511	0.01432	0.04112	2.87
ABCD1	NM_007435	0.01004	0.03760	3.74
ABCD2	NM_011994	0.00233	0.02212	9.48
ABCD3	**NM_008991**	**0.00015**	**0.01411**	**89.65**
ABCD4	**NM_008992**	**0.00002**	**0.0016**	**80**
ABCF1	XM_128626	0.00724	0.02650	3.66
ABCF3	NM_013852	0.00666	0.02689	4.04
Phase II: glutathione S-transferases				
CHST1	NM_023850	0.08887	0.02998	0.34
CHST4	NM_011998	0.04060	0.01555	0.38
CHST5	NM_019950	0.02198	0.00957	0.44
CHST3	NM_016803	0.00650	0.01778	2.73
Phase I: P450 Gene Family				
CYP19	NM_007810	0.00212	0.01669	7.86
CYP40	XM_125908	0.00899	0.01821	2.02
CYP7b1	NM_007825	0.00089	0.00300	3.37
CYP8b1	NM_010012	0.00175	0.03037	17.28
CYP17	NM_007809	0.02442	0.01012	0.41
CYP2a4	NM_009997	0.00802	0.00363	0.45
CYP4b1	NM_007823	0.03074	0.01219	0.40
Acetyltransferases				
N-Acetyltransferase	NM_008673	0.03457	0.01622	0.47
Phase II: glutathione S-transferases				
GSTP1	**NM_013541**	**0.04851**	**0.00534**	**0.11**
GSTT1	NM_008185	0.03538	0.00617	0.17
GSTT2	NM_010361	0.03245	0.00777	0.23

anion. The results of *in vitro* accumulation and efflux experiments indicated that when mouse primary hepatocytes reached a saturation uptake of PLA–PEG nanoparticles during the concentration range of 750–1000 μg/ml, about 51–52% (51.5% and 52.0%) intracellular nanoparticles was expulsed by mouse primary hepatocytes. We suggested that a part of nanoparticles may form a compound (GS-X) with GSH molecules, and this compound be pumped out by MRP5 in order to protect normal physiologic function of cells. Cells showed resistance to excessive PLA–PEG nanoparticles via one or more of several mechanisms. After high amount of PLA–PEG nanoparticles was internalized by hepatic cells, a part of nanoparticles were hydrolyzed into oligomers, and these polymers after hydrolysis were pumped out by some ABC transporters (especially ABCA8) using the energy of ATP hydrolysis. Other PLA–PEG nanoparticles conjugated with glutathione (GSH) would be transported out of cells by MRP5 (Fig. 6).

In the result of gene expression analysis, expression of ABCC5 in treated group increased as 92.48-fold change compared with that of control group. In contrast, despite its general up-regulation in cancer cells, GSTP1 which catalyzes the conjugation of glutathione to drugs was significantly down-regulated in liver of mouse. We next sought to determine whether the differential expression of ABCC5 (MRP5) and GSTP1 could be confirmed by RT-PCR. The results showed that ABCC5 (MRP5) was over-expressed and GSTP1 was down-regulated in the nanoparticles treated mouse (Fig. 7, Table 4). Annereau et al. also demonstrated that ABC transporters (ABCB1/MDR1 and ABCC2/MRP2, respectively) showed dramatic overexpression, whereas the glutathione *S*-transferase gene GSTP1 showed the strongest expression decrease in the study of RCO.1 cell line's multidrug resistance to camptothecin analogs [43]. Model (Fig. 6) depicted MRP5-mediated transport of PLA–PEG nanoparticles across the cell

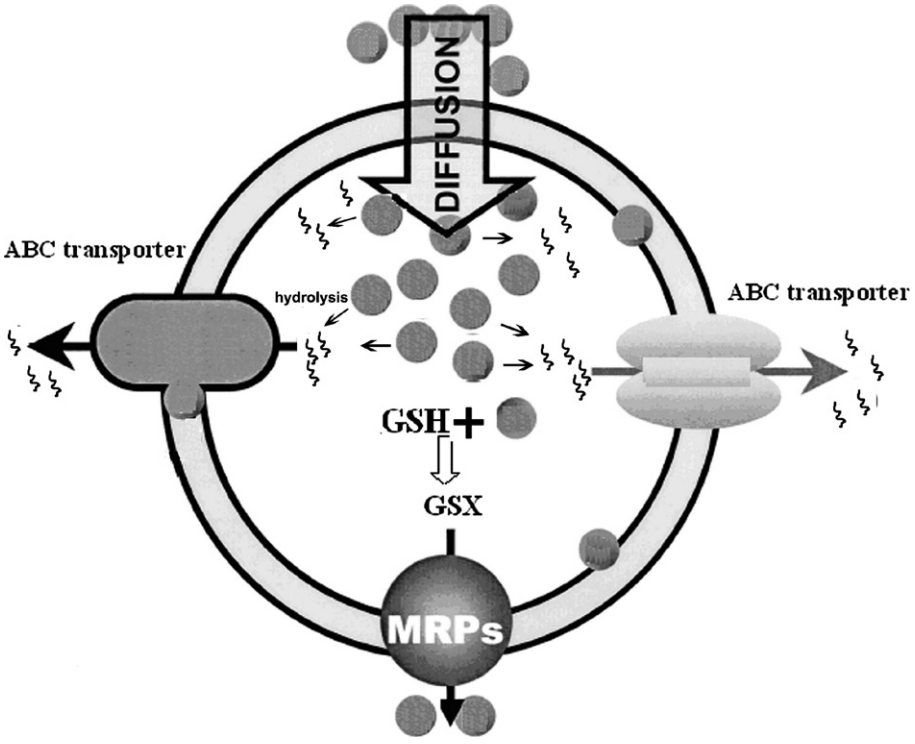

Fig. 6. ABC transporters pumped out low molecular weight polymers (small arrow) after nanoparticles hydrolysis and MRP5 (ABCC5) expulsed a part of PLA–PEG nanoparticles from mouse hepatic cells.

membrane. The contrary reduction of GSTP1 in hepatic cells of mouse was the most striking of the seemingly paradoxical changes that we observed. So we next consider this unexpected phenomenon.

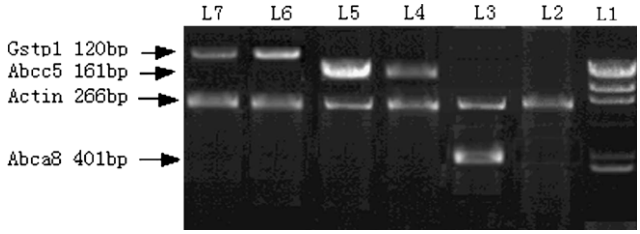

Fig. 7. Kunming mice received PEG–PLA nanoparticles solution injection via the tail vein (42.04 mg/kg, i.v.), after 4 days mice were killed. Total RNA of liver was isolated and subjected to RT-PCR analysis. (A) The PCR products of ABCA8 (401 bp), Actin (266 bp), GSTP1 (120 bp) and ABCC5 (161 bp) were visualized by electrophoresis on an agarose gel containing ethidium bromide: lane 1, marker; lane 2, ABCA8 (401 bp) of moderate dose treated mice; lane 3, ABCA8 (401 bp) of untreated mice; lane 4, ABCC5 (161 bp) of large dose treated mice; lane 5, ABCC5 (161 bp) of untreated mice; lane 6, GSTP1 (120 bp) of untreated mice; lane 7, GSTP1 (120 bp) of large dose treated mice.

Table 4
Densitometric analysis of RT-PCR products

Group	ABCA8	ABCC5	GSTT1
Large dose treated	0.2	4.3	0.13
Control	0	0.02	1.6

Each value of mRNA level was normalized with actin beta mRNA level.

3.6.4. Gene expression differences in GSTP1

GSTP1 *is* one member of glutathione *S*-transferase (GST) family that catalyze the conjugation of glutathione with a number of electrophilic compounds [44]. GSTP1 was markedly suppressed in hepatic cells of mouse (large dose treated/control = 0.13 by Microarray; 0.081 by RT-PCR). GSTP1 protects cells against apoptosis induced by oxidative stress or DNA damaging drugs [45]. Therefore, the markedly reduced GSTP1 mRNA level in hepatic cells was in the contrary direction.

In our experiment, mice were injected with large dose of PLA–PEG nanoparticles, accumulation of PLA–PEG nanoparticles in mouse liver took place. Like RCO.1 cells gained resistance to camptothecin by maintaining with passage in camptothecin-containing medium [43,46]. Mouse hepatic cells exposed to PLA–PEG nanoparticles chronically had resistance to these nanoparticles by suppressing GSTP1 expression, as PLA–PEG nanoparticles had long blood circulation. Former papers suggest that an AP-1 site of the GSTP1 promoter can be activated by Fra-1: c-Jun heterodimer [47]. Thus, the reduced GSTP1 mRNA level may have been attributable in part to lower Fra-1 mRNA. Fra-1 has a transactivation domain that can be activated through phosphorylation by ERK [46,48].

4. Conclusions

This work reported the effect of blank PLA–PEG nanoparticles on hepatic cells of mouse. Diameter

well-controlled PLA–PEG nanoparticles could be prepared by emulsion solvent evaporation technique. MTT assay showed that PLA–PEG nanoparticles had low cytotoxicity in controlled concentration range (0.001–0.1 mg/ml). Biochemical analysis of MDA level, NOS activity and SOD activity demonstrated that large dose of PLA–PEG nanoparticles injection did not induce cell damage of liver, kidney, heart, and serum. Immunohistochemical analysis of liver, heart, and kidney suggested that large dose of PLA–PEG nanoparticles injection could not induce cell apoptosis. *In vitro* accumulation and efflux experiments showed that about 51–52% (51.5% and 52.0%) intracellular nanoparticles was expulsed by mouse primary hepatocytes after the cell reached a saturation uptake of PLA–PEG nanoparticles during the concentration range of 750–1000 μg/ml. Microarray analysis of gene expression of mouse liver showed overexpression of ABCA8, ABCC5/MRP5 and down-regulation of GSTP1. ABCA8 protein was very important in efflux of polymers after nanoparticles hydrolysis from mouse hepatic cells which reached saturation uptake of these nanoparticles. ABCC5 expressed multidrug resistance protein 5 (MRP5) to extrude conjugate GS-X outside mouse hepatic cells. The results were confirmed by RT-PCR. The overcoming of mouse hepatic cell multidrug resistance to PLA–PEG nanoparticles will be investigated in our further studies.

Acknowledgments

We thank Kangchen Bio-tech Company for technical advice on cDNA array technical service. This work was supported by National Natural Science Foundation of China (No. 30400185), the National High Technology Research and Development Project of China (No. 2002AA216011) and the Major State Basic Research Development Program of China (No. 2004CB518802).

References

[1] D. Bazile, C. Prud'homme, M.T. Bassoullet, M. Marlard, G. Spenlehauer, M. Veillard, Stealth Me.PEG–PLA nanoparticles avoid uptake by the mononuclear phagocytes system, J. Pharm. Sci. 84 (1995) 493–498.

[2] C.A. Nguyen, E. Allemann, G. Schwach, E. Doelker, R. Gurny, Cell interaction studies of PLA-MePEG nanoparticles, Int. J. Pharm. 254 (2003) 69–72.

[3] R. Gref, P. Quellec, A. Sanchez, P. Calvo, E. Dellacherie, M.J. Alonso, Development and characterization of CyA-loaded poly(lactic acid)-poly(ethylene glycol) PEG micro- and nanoparticles. Comparison with conventional PLA particulate carriers, Eur. J. Pharm. Biopharm. 51 (2001) 111–118.

[4] Z. Panagi, A. Beletsi, G. Evangelatos, E. Livaniou, D.S. Ithakissios, K. Avgoustakis, Effect of dose on the biodistribution and pharmacokinetics of PLGA and PLGA-mPEG nanoparticles, Int. J. Pharm. 221 (2001) 143–152.

[5] A. Vila, H. Gill, O. McCallion, M.J. Alonso, Transport of PLA–PEG particles across the nasal mucosa: effect of particle size and PEG coating density, J. Control Release 98 (2004) 231–244.

[6] N. Saito, T. Okada, H. Horiuchi, N. Murakami, J. Takahashi, M. Nawata, H. Ota, S. Miyamoto, K. Nozaki, K. Takaoka, Biodegradable poly-D,L-lactic acid-polyethylene glycol block copolymers as a BMP delivery system for inducing bone, J. Bone Joint Surg. Am. 83-A (Suppl. 1) (2001) S92–S98.

[7] N. Tamai, A. Myoui, M. Hirao, T. Kaito, T. Ochi, J. Tanaka, K. Takaoka, H. Yoshikawa, A new biotechnology for articular cartilage repair: subchondral implantation of a composite of interconnected porous hydroxyapatite, synthetic polymer (PLA–PEG), and bone morphogenetic protein-2 (rhBMP-2), Osteoarthritis Cartilage 13 (2005) 405–417.

[8] T. Kaito, A. Myoui, K. Takaoka, N. Saito, M. Nishikawa, N. Tamai, H. Ohgushi, H. Yoshikawa, Potentiation of the activity of bone morphogenetic protein-2 in bone regeneration by a PLA–PEG/hydroxyapatite composite, Biomaterials 26 (2005) 73–79.

[9] V.L. Colvin, The potential environmental impact of engineered nanomaterials, Nat. Biotechnol. 21 (2003) 1166–1170.

[10] K. Donaldson, V. Stone, A. Clouter, L. Renwick, W. MacNee, Ultrafine particles, Occup. Environ. Med. 58 (199) (2001) 211–216.

[11] G. Oberdorster, E. Oberdorster, J. Oberdorster, Nanotoxicology: an emerging discipline evolving from studies of ultrafine particles, Environ. Health Perspect. 113 (2005) 823–839.

[12] R.F. Service, Nanotoxicology. Nanotechnology grows up, Science 304 (2004) 1732–1734.

[13] K.Y. Win, S.S. Feng, Effects of particle size and surface coating on cellular uptake of polymeric nanoparticles for oral delivery of anticancer drugs, Biomaterials 26 (2005) 2713–2722.

[14] J. Panyam, V. Labhasetwar, Dynamics of endocytosis and exocytosis of poly(D,L-lactide-co-glycolide) nanoparticles in vascular smooth muscle cells, Pharm. Res. 20 (2003) 212–220.

[15] Y.Y. Chiu, K. Higaki, B.L. Neudeck, J.L. Barnett, L.S. Welage, G.L. Amidon, Human jejunal permeability of cyclosporin A: influence of surfactants on P-glycoprotein efflux in Caco-2 cells, Pharm. Res. 20 (2003) 749–756.

[16] B.M. Johnson, W.N. Charman, C.J. Porter, An in vitro examination of the impact of polyethylene glycol 400, Pluronic P85, and vitamin E d-alpha-tocopheryl polyethylene glycol 1000 succinate on P-glycoprotein efflux and enterocyte-based metabolism in excised rat intestine, AAPS PharmSci. 4 (2002) E40.

[17] E.M. Collnot, C. Baldes, M.F. Wempe, J. Hyatt, L. Navarro, K.J. Edgar, U.F. Schaefer, C.M. Lehr, Influence of vitamin E TPGS poly(ethylene glycol) chain length on apical efflux transporters in Caco-2 cell monolayers, J. Control Release 111 (2006) 35–40.

[18] L.B. Moore, B. Goodwin, S.A. Jones, G.B. Wisely, C.J. Serabjit-Singh, T.M. Willson, St. John's wort induces hepatic drug metabolism through activation of the pregnane X receptor, Proc. Natl. Acad. Sci. USA 13 (2000) 7500–7502.

[19] V.C. Mosqueira, P. Legrand, J.L. Morgat, M. Vert, E. Mysiakine, R. Gref, J.P. Devissaguet, G. Barratt, Biodistribution of long-circulating PEG-grafted nanocapsules in mice: effects of PEG chain length and density, Pharm. Res. 18 (2001) 1411–1419.

[20] Y.Z. Zhiyuan Hu, Jiwei Wang, Yifeng Pan, Denggao Zhai, Liang Tan, Yulin Luo, Preparation of epirubicin-loaded PLA–PEG nanoparticles and technical optimization, Nanoscience 1 (2005) 135–139.

[21] B.L. Kreamer, J.L. Staecker, N. Sawada, G.L. Sattler, M.T. Hsia, H.C. Pitot, Use of a low-speed, iso-density percoll centrifugation method to increase the viability of isolated rat hepatocyte preparations, In Vitro Cell. Dev. Biol. 22 (1986) 201–211.

[22] T. Sasada, S. Iwata, N. Sato, Y. Kitaoka, K. Hirota, K. Nakamura, A. Nishiyama, Y. Taniguchi, A. Takabayashi, J. Yodoi, Redox control of resistance to cis-diamminedichloroplatinum (II) (CDDP): protective effect of human thioredoxin against CDDP-induced cytotoxicity, J. Clin. Invest. 97 (1996) 2268–2276.

[23] Y. Sun, L.W. Oberley, Y. Li, A simple method for clinical assay of superoxide dismutase, Clin. Chem. 34 (1988) 497–500.

[24] H. Esterbauer, K.H. Cheeseman, Determination of aldehydic lipid peroxidation products: malonaldehyde and 4-hydroxynonenal, Methods Enzymol. 186 (1990) 407–421.

[25] S.M. Read, D.H. Northcote, Minimization of variation in the response to different proteins of the Coomassie blue G dye-binding assay for protein, Anal. Biochem. 116 (1981) 53–64.
[26] J. Panyam, J. Lof, E. O'Leary, V. Labhasetwar, Efficiency of dispatch and infiltrator cardiac infusion catheters in arterial localization of nanoparticles in a porcine coronary model of restenosis, J. Drug Target. 10 (2002) 515–523.
[27] M. Tobio, R. Gref, A. Sanchez, R. Langer, M.J. Alonso, Stealth PLA–PEG nanoparticles as protein carriers for nasal administration, Pharm. Res. 15 (1998) 270–275.
[28] W.J. Lin, Y.C. Chen, C.C. Lin, C.F. Chen, J.W. Chen, Characterization of pegylated copolymeric micelles and in vivo pharmacokinetics and biodistribution studies, J. Biomed. Mater. Res. B. Appl. Biomater. 77 (2006) 188–194.
[29] A. Baldan, P. Tarr, R. Lee, P.A. Edwards, ATP-binding cassette transporter G1 and lipid homeostasis, Curr. Opin. Lipidol. 17 (2006) 227–232.
[30] W. Jessup, I.C. Gelissen, K. Gaus, L. Kritharides, Roles of ATP binding cassette transporters A1 and G1, scavenger receptor BI and membrane lipid domains in cholesterol export from macrophages, Curr. Opin. Lipidol. 17 (2006) 247–257.
[31] S. Li, Hydrolytic degradation characteristics of aliphatic polyesters derived from lactic and glycolic acids, J. Biomed. Mater. Res. 48 (1999) 342–353.
[32] D.V. Bazile, C. Ropert, P. Huve, T. Verrecchia, M. Marlard, A. Frydman, M. Veillard, G. Spenlehauer, Body distribution of fully biodegradable [14C]-poly(lactic acid) nanoparticles coated with albumin after parenteral administration to rats, Biomaterials 13 (1992) 1093–1102.
[33] P. Quellec, R. Gref, L. Perrin, E. Dellacherie, F. Sommer, J.M. Verbavatz, M.J. Alonso, Protein encapsulation within polyethylene glycol-coated nanospheres. I. Physicochemical characterization, J. Biomed. Mater. Res. 42 (1998) 45–54.
[34] T.M. Chang, Therapeutic applications of polymeric artificial cells, Nat. Rev. Drug Discov. 4 (2005) 221–235.
[35] W.P. Yu, T.M. Chang, Submicron polymer membrane hemoglobin nanocapsules as potential blood substitutes: preparation and characterization, Artif. Cells Blood Substit. Immobil. Biotechnol. 24 (1996) 169–183.
[36] Y. Nakae, P.J. Stoward, The initial reaction velocities of lactate dehydrogenase in various cell types, Histochem. J. 26 (1994) 283–291.
[37] M. Wakaumi, K. Ishibashi, H. Ando, H. Kasanuki, S. Tsuruoka, Acute digoxin loading reduces ABCA8A mRNA expression in the mouse liver, Clin. Exp. Pharmacol. Physiol. 32 (2005) 1034–1041.
[38] J. Wijnholds, C.A. Mol, L. van Deemter, M. de Haas, G.L. Scheffer, F. Baas, J.H. Beijnen, R.J. Scheper, S. Hatse, E. De Clercq, J. Balzarini, P. Borst, Multidrug-resistance protein 5 is a multispecific organic anion transporter able to transport nucleotide analogs, Proc. Natl. Acad. Sci. USA 97 (2000) 7476–7481.
[39] P. Borst, R. Evers, M. Kool, J. Wijnholds, A family of drug transporters: the multidrug resistance-associated proteins, J. Natl. Cancer Inst. 92 (2000) 1295–1302.
[40] S.P. Cole, R.G. Deeley, Multidrug resistance mediated by the ATP-binding cassette transporter protein MRP, Bioessays 20 (1998) 931–940.
[41] M.A. McAleer, M.A. Breen, N.L. White, N. Matthews, pABC11 (also known as MOAT-C and MRP5), a member of the ABC family of proteins, has anion transporter activity but does not confer multidrug resistance when overexpressed in human embryonic kidney 293 cells, J. Biol. Chem. 274 (1999) 23541–23548.
[42] G. Rappa, A. Lorico, R.A. Flavell, A.C. Sartorelli, Evidence that the multidrug resistance protein (MRP) functions as a co-transporter of glutathione and natural product toxins, Cancer Res. 57 (1997) 5232–5237.
[43] J.P. Annereau, G. Szakacs, C.J. Tucker, A. Arciello, C. Cardarelli, J. Collins, S. Grissom, B.R. Zeeberg, W. Reinhold, J.N. Weinstein, Y. Pommier, R.S. Paules, M.M. Gottesman, Analysis of ATP-binding cassette transporter expression in drug-selected cell lines by a microarray dedicated to multidrug resistance, Mol. Pharmacol. 66 (2004) 1397–1405.
[44] I. Hatayama, K. Satoh, K. Sato, A cDNA sequence coding a class pi glutathione *S*-transferase of mouse, Nucleic Acids Res. 18 (1990) 4606.
[45] S. Goto, Y. Ihara, Y. Urata, S. Izumi, K. Abe, T. Koji, T. Kondo, Doxorubicin-induced DNA intercalation and scavenging by nuclear glutathione *S*-transferase pi, FASEB J. 15 (2001) 2702–2714.
[46] W.C. Reinhold, H. Kouros-Mehr, K.W. Kohn, A.K. Maunakea, S. Lababidi, A. Roschke, K. Stover, J. Alexander, P. Pantazis, L. Miller, E. Liu, I.R. Kirsch, Y. Urasaki, Y. Pommier, J.N. Weinstein, Apoptotic susceptibility of cancer cells selected for camptothecin resistance: gene expression profiling, functional analysis, and molecular interaction mapping, Cancer Res. 63 (2003) 1000–1011.
[47] P. Borde-Chiche, M. Diederich, F. Morceau, M. Wellman, M. Dicato, Phorbol ester responsiveness of the glutathione *S*-transferase P1 gene promoter involves an inducible c-jun binding in human K562 leukemia cells, Leuk. Res. 25 (2001) 241–247.
[48] M.R. Young, R. Nair, N. Bucheimer, P. Tulsian, N. Brown, C. Chapp, T.C. Hsu, N.H. Colburn, Transactivation of Fra-1 and consequent activation of AP-1 occur extracellular signal-regulated kinase dependently, Mol. Cell. Biol. 22 (2002) 587–598.